Cyclohexanedione as the negative electrode reaction for organic redox flow batteries

P. Leung[a,b,†], T. Martin[a], M. Liras[a], A.M. Berenguer[a], R. Marcillia[a], A. Shah[c,*], M.A. Anderson[a,c], J. Palma[a]

a. IMDEA Energy Institute, Mostoles, Spain.

b. Department of Materials, University of Oxford, Oxford, United Kingdom.

c. School of Engineering, University of Warwick, Coventry CV47AL, United Kingdom

d. Environmental Chemistry & Technology Program, University of Wisconsin-Madison, United States.

† puiki.leung@materials.ox.ac.uk; * akeel.shah@warwick.ac.uk

Abstract

The electrochemical reduction and oxidation of cyclohexanedione is evaluated for the first time as the negative electrode reaction in an organic redox flow battery. Electrochemical characterization indicates that the redox reaction of cyclohexanedione is a proton-coupled electron transfer process with quasi-reversible behaviour in acidic media (pH < 3). Among three isomeric compounds (1,2-, 1,3- and 1,4-cyclohexanedione), the reduction of 1,3-cyclohexanedione exhibits the most negative electrode potential (*c.a.* –0.6 V *vs.* Ag|AgCl (*c.a.* –0.4 V *vs.* NHE)) as well as the widest pH operating range (pH 1 – 5) for relatively reversible reactions. The resulting electrode potential is the most negative of those to have been reported in neutral/acidic electrolytes. 1,3-cyclohexanedione is subsequently used as the active species in the negative electrode of a parallel plate flow cell, which is charge-discharge cycled at 3.4 mA cm^{-2} for 100 cycles, yielding half-cell coulombic efficiencies of *c.a.* 99 %. The organic molecules derived from this group are observed to have high solubilities (> 2 M) and exhibit reduction process with up to 4 electrons transferred.

Keywords: Cyclohexanedione, negative electrode, organic, redox flow batteries, soluble.

Introduction

The European Union commission has set a target of a 43 % reduction in greenhouse gas emissions from all sectors by 2030 (from the 2005 level) [1]. Achieving this and similar targets adopted in other regions of the world will require the wide-scale deployment of renewable power sources in grid-scale and transport applications [2]. In order to facilitate the penetration of intermittent renewables into power grids (provide flexible and stable energy outputs to end-users), it is commonly accepted that efficient and competitively priced energy storage systems will play a major role [3–10].

In the past few decades, a number of energy storage technologies have been developed and successfully demonstrated. Amongst these technologies, electrochemical devices are considered to be attractive since they can be installed in any location (not terrain dependent in contrast to pumped-hydro and compressed air), do not involve any disruption to the environment and do not involve very high capital costs [5–6]. To ensure that energy storage devices are economically viable in long term, the Department of Energy of the United States (DoE) has set a system capital cost target of USD$ 150 / kWh by 2023, to match with the operating costs of existing physical energy storage technologies [7-11].

Considering their potential economic and safety advantages, redox flow batteries are recognized as the most realistic candidates for storage in the range of a few kW/ kWh up to tens of MW / MWh. In contrast to conventional rechargeable batteries, redox flow batteries store energy in the form of reduced and oxidized electroactive species in flowing electrolytes and/or on the electrode surfaces, while conventional batteries (e.g.. lead acid and lithium-ion batteries) contain static electrolytes and store energy within the electrode structures [5]. For flow batteries, the power output and energy capacity can be adjusted readily by increasing the electrode size or/and the electrolyte volume.

Since the invention of the redox flow battery concept, various chemistries based on metallic active materials (i.e. all-vanadium [12], zinc-cerium [13], vanadium-cerium [14] and all-copper [15]) have been proposed. The all-vanadium redox flow battery is the most developed and widely studied system due to its high reversibility and relatively large power output. In relation to the DoE target (USD$ 150 / kWh), the capital costs of vanadium systems are, however, still too high (USD$ 200 – 750 / kWh) for extensive market penetration [16]. For example, the electrolyte cost of the vanadium redox flow batteries exceeds USD$ 80 / kWh [17].

In order to reduce costs (especially those of the electrolytes), recent investigations have proposed the use of organic active materials. In general, organic molecules are abundant and can be extracted readily from various sources. Even in the early stage of development, the electrolyte cost of the organic flow battery has been demonstrated to be lower than USD$ 35 / kWh (for the redox couples of anthraquinone / benzoquinone or anthraquinone/ bromine) [18, 19].

The electrolyte cost per kWh can be further decreased by selecting the most suitable active materials with regards to the resulting cell voltages or/and multi-electron transfers. At the same time, the selected organic molecules should provide reasonable energy densities (Wh dm^{-3}) by maintaining high solubilities in particular solvents. In the past few years, several organic compounds, including the derivatives of 2,5-di-tert-butyl-1,4,bis(2-methoxyethox)benzene (DBBB) [20, 21], quinoxaline [22, 23] and (2,2,6,6-tetramethylpiperidin-1-yl)oxyl (TEMPO) [24], have been evaluated in non-aqueous solvents (i.e. propylene carbonate, acetonitrile). Despite the wider electrochemical stability windows (> 1.3 V) and the possibility of higher solubilities, non-aqueous solvents tend to be volatile and moisture sensitive [25]. The ionic conductivities of these pure solvents (e,g,. 1×10^{-8} S cm^{-1} for propylene carbonate; 6×10^{-10} S cm^{-1} for acetonitrile) are significantly lower than

76 that of water (6×10^{-8} S cm^{-1}) [25]. Furthermore, the cost of non-aqueous solvents (e.g.
77 USD$ 1.5 – 1.7 per dm^{-3} for propylene carbonate [26]) and their salts (particularly,
78 fluorinated salts) can be a factor of several hundred times more expensive than water (<
79 USD$ 0.004 per dm^{-3} [27]) for industrial applications. For these reasons, the aim of this work
80 is to develop organic redox flow batteries based on aqueous electrolytes.

81 In recent years, a number of aqueous chemistries with high energy contents have been
82 introduced for energy storage applications [28 – 32]. For the case of redox flow batteries,
83 there have been few studies of the use of organic molecules [33 – 41], particularly quinone-
84 based molecules, for the electrode reactions. The prototypical member of the quinone
85 molecule is 1,4-benzoquinone, which is also known as cyclohexadienedione. The
86 corresponding redox reactions in aqueous electrolytes are expressed as follow:

87 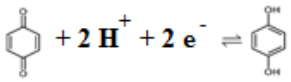 (1)

88 The resulting chemistries involve at least one proton and one electron by forming hydroxyl
89 group(s) (OH-), which result in the transformation of hydroquinone molecules. Such
90 hydroxyl groups not only serve as the liquid carriers of hydrogen for energy conversion [42]
91 but also enhance the solubilities in aqueous electrolytes [43]. The selection of quinone
92 molecules, including benzoquinones, naphthoquinones and anthraquinones, has been
93 facilitated by computational screening within the framework of the density functional theory
94 (DFT), by evaluating the equilibrium potentials and the solubilities of up to 1700 quinone-
95 based redox couples [43]. Unless the functional groups were modified, the equilibrium
96 potentials of the parent isomers of these quinone molecules were between + 0.05 and + 1.1 V
97 vs. SHE. These previous investigations [43] suggest that the 9-10-anthraquinone (E_0 = + 0.1
98 V *vs.* SHE) is the most suitable redox couple for the negative electrode, whereas the 1,2-

benzoquinone, 2,3-naphthoquinones and 2,3-anthraquinone ($E_0 \geq +0.7$ V *vs.* SHE) are reasonable candidates for the positive electrode reactions.

The resulting quinone-based molecules have been tested experimentally in redox flow batteries by two research groups (Harvard [19, 35] and Southern California Universities [33]) in the United States. Both research groups proposed different battery chemistries based on metal-free compounds (Harvard: anthraquinone/bromine; Southern California: anthraquinone/ benzoquinone) but used the derivatives of the 9, 10-anthraquinone molecules as the negative electrode reactions. The redox potentials of these molecules ($E_0 \geq c.a. + 0.1$ V *vs.* SHE) are still rather too positive, however, to be used as the negative electrode reactions. On the other hand, more than 300 quinones were predicted to have electrode potentials of above 0.7 V *vs.* SHE, which tend to be more positive in neutral/acidic electrolytes, and are therefore suitable for the positive electrode reaction [42].

Furthermore, the reported anthraquinone molecules with sulfonic acid and hydroxyl substituents have solubilities of around 1.0 mol dm^{-3} (9, 10-anthraquinone-2, 7-disulphonic acid: 1.0 mol dm^{-3} [19]; 9, 10-anthraquinone-2, 6-disulphonic acid: 0.5 mol dm^{-3} [33], 9, 10-anthraquinone-2-sulphonic acid: 0.2 mol dm^{-3} [33]) and even less in the un-substituted forms (< 0.2 mol dm^{-3}). For the development of organic redox flow batteries, it is important to search for alternative redox couples that offer negative electrode potentials and reasonable solubilities (i.e. > 0.5 mol dm^{-3}). Amongst the various organic compounds, in this work we investigate the possibility of using cyclohexanedione for the negative electrode reaction in redox flow batteries. The proposed organic compound is a simple molecule (molecular weight: 112 g mol^{-1}), similar to benzoquinone in terms of molecular structure, which exhibits two hydroxyl groups for energy conversion. The low molecular weight of this molecule suggests the highest theoretical specific capacities (474 A h Kg^{-1} (2 e^- transfers); 948 A h Kg^-

[1] (4 e^- transfers)) among all the organic molecules used in the negative electrolytes (Table S1 in Supplementary Information).

As documented in the field of organic chemistry [44 – 46], the redox reactions of the three isomeric cyclohexanediones undergo proton-coupled electron transfer, and transform to cyclohexanediol structures:

1, 2- cyclohexanedione:

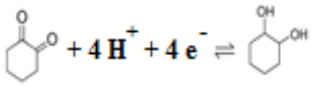

(2)

1, 3- cyclohexanedione:

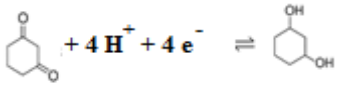

(3)

1, 4- cyclohexanedione:

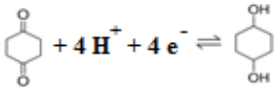

(4)

The physical and electrochemical properties vary among the three isometric compounds. In aqueous solutions, the solubilities of the 1,2-, 1,3-, and 1,4-cyclohexanediones are 2.5, 2.0, 5.2 mol dm^{-3}, respectively. The solubilities of the reduced species are expected to be even higher due to the presence of the hydroxyl functional groups. In fact, the described solubility of 1,4-cyclohexanediol is up to 13.5 mol dm^{-3}. Without functionalization, the solubilities of these compounds are significantly higher than those of benzoquinones (i.e. 1,4-benzoquinone: 0.1 mol dm^{-3}; 1,4-hydroquinone: 0.6 mol dm^{-3}). The electrochemical properties of these compounds have been reported by a few studies in biological and

electroanalytical chemistries [44 – 46]. Together with high dehydrogenation energy (14.9 – 15.8 kCal per mole of hydrogen) calculated using density functional theory (DFT) [42], voltammetric studies show that the redox potentials of these molecules are more negative than – 0.1 V *vs.* SHE [47 – 52], which makes them attractive as the negative redox couples for organic redox flow batteries. Therefore, the objective of this work is to improve the understanding of the electrochemical behaviour of the cyclohexanedione compounds, which can act as alternatives for energy storage applications. Half-cell electrochemical studies, including cyclic voltammetry and galvanostatic charge-discharge experiments, were used to characterize the redox reaction and to demonstrate the cycling performance in a parallel-plate redox flow battery.

2. Experimental

2.1. Chemicals

Analytical grade 1,2-, 1,3-, and 1,4-cyclohexanedione, 1,4-cyclohexanediol, 1,4-benzoquinone, 1,4-hydroquinone, sodium chloride, sodium hydroxide and the reagent grade aqueous hydrochloric acid were supplied from Sigma Aldrich (Germany) and Fisher Scientific (United Kingdom). The gas chromatography-mass spectrometry of the 1,2-, 1,3- and 1,4- cyclohexanedione is summarized in Table S2 (Supplementary Information). Solutions were prepared with ultra-pure water (18 MΩ cm resistivity) from a Millipore water purification system (Milli-Q Integral 3). Typical electrolytes contained 0.010 mol dm^{-3} and 0.2 mol dm^{-3} active materials for the cyclic voltammetry and the charge-discharge experiments, respectively. Supporting solutions were 0.2 mol dm^{-3} sodium chloride adjusted at specified pH using sodium hydroxide or hydrochloric acid aqueous solutions.

2.2. Cyclic voltammetry/ Linear sweep voltammetry

A typical three-electrode glass cell with approximately 20 cm^3 electrolyte volume was used for the cyclic voltammetry experiments, in which the working electrodes were either platinum or glassy carbon. Counter and reference electrodes were platinum and silver-silver chloride (ST 612 Radiometer Analytical SA, France, 3 M KCl) [53, 54]. Potentials in all measurements can be transformed into the normal hydrogen electrode potential (NHE) scale by adding 205 mV to the reference electrode readings (e.g.. 0 V *vs*. Ag|AgCl can be reported as +0.205 V *vs*. NHE).

In typical tests, electrode potential measurements were made using a Bio-logic VMP potentiostat (Bio-logic SAS, France) over a wide range of electrolyte compositions including 0.01 – 0.2 mol dm^{-3} active material in a supporting electrolyte of 0.2 mol dm^{-3} sodium chloride adjusted to particular pH (pH 1 – 11) with hydrochloric acid/ sodium hydroxide solutions. For the case of cyclohexanedione, the potential of the working electrode was swept between – 0.10 and – 1.15 V *vs.* Ag|AgCl at a potential sweep rate in the range 4 to 100 mV s^{-1}. To evaluate the effect of mass transport, linear sweep voltammetry was conducted in a rotating disk electrode set-up at various speeds: 100, 225, 400, 625, 900, 1600 and 2500 rpm.

2.3. Half-cell galvanostatic charge-discharge cycling

The reduction and oxidation reactions of the 1,3-cyclohexanedione active compounds were carried out in a divided parallel-plate flow cell. A cation-conducting Nafion® membrane (Dupont, NF117/ H^+) was used to separate the two compartments [55, 56]. Platinized titanium electrodes (2.5 cm × 2.5 cm, 2.5 μm coating, Ti-shop.com, United Kingdom) were used for both the negative and positive electrode reactions. Each electrode had an area of 2.5 cm × 2.5 cm with a gap of 2.0 cm between the electrode surface and the membrane. The volume of each electrolyte contained in separated tanks was 18 cm^3. The negative and positive electrolytes were circulated through the cell at a mean linear flow velocity between

0.34 and 0.90 cm^3 s^{-1}. The two electrolytes contained 0.2 mol dm^{-3} 1,3-cyclohexanedione and 0.2 mol dm^{-3} sodium hydroxide solution and were controlled at 298 K by a thermostat through two double walled water jackets. The reference electrode was silver-silver chloride, placed at the entrance of each channel, in line with the electrolyte circuit. The negative electrolytes were initially reduced to the equilibrium potentials of the relevant electrode reactions ($E_0 \approx$ *c.a.* – 0.5 V *vs.* Ag|AgCl at pH 3.5) and purged with a fast stream of pure nitrogen to minimize the oxidation of the reduced species with atmospheric air. In a typical charge-discharge cycling experiment, negative and positive current densities of 3.2 mA cm^{-2} (20 mA) were applied at the working electrodes, for the reduction and oxidation of the cyclohexanedione molecules. The upper voltage limits were controlled at 300 mV more positive from the open-circuit potential measured before the subsequent discharge cycle. The half-cell coulombic efficiencies were obtained as follows:

$$\text{Half-cell coulombic efficiency} = I_d\, t_d / I_c\, t_c \times 100\ \% \quad (5)$$

in which I is the applied current density during charge/discharge, t is the duration of charge/discharge, and the subscripts c and d denote the charge and discharge processes, respectively. In some experiments, the reactants and products were analyzed off-line by gas chromatography-mass spectrometry (GCMS, Bruker, BP-5 ms; 5 % diphenyl/ 95 % dimethyl polysiloxane column).

3. Results and Discussion

3.1. Electrochemical Characterizations of Cyclohexanedione Molecules in Sodium Chloride Solutions

3.1.1. Cyclic Voltammetry of Cyclohexanedione Molecules

The electrochemical characterization of the prototypical 1,4-cyclohexanedione was performed using cyclic voltammetry in 0.2 mol dm^{-3} sodium chloride solutions. Figure 1

shows the voltamograms of this molecule under a wide potential range between – 2.0 and + 1.6 V *vs*. Ag|AgCl using platinum and carbon electrodes.

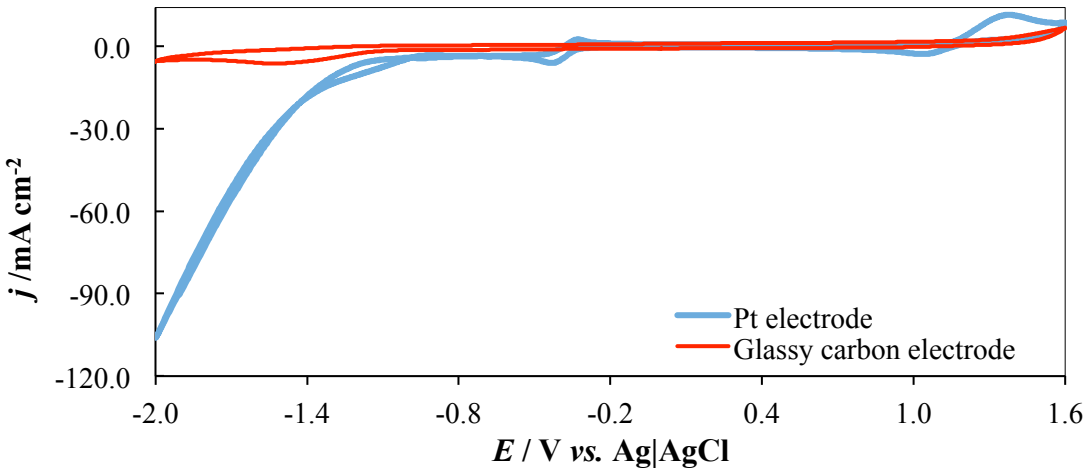

Figure 1

Fig. 1. Cyclic voltammograms for the reduction of 10 mmol dm^{-3} cyclohexanedione in 0.2 mol dm^{-3} sodium chloride solution (pH 2) at platinum and glassy carbon; Temperature = 25 ^{o}C; potential sweep rate: 100 mV s^{-1}. The NHE potential scale is obtained by adding 205 mV from Ag|AgCl reference readings.

Compared to the glassy carbon electrode, the reaction current densities at platinum electrodes are significantly higher. Moreover, two pairs of reactions were observed to be reversible/quasi-reversible in both regions of negative and positive potentials. The cyclic voltammetry on glassy carbon does not exhibit any reversible peak, indicating that catalysts are necessary for the redox reaction processes. These results are similar to those obtained in the reduction of the 1,2- and 1,3- cyclohexanedione molecules using metallic electrodes, such as mercury [47, 48] and stainless steel [51].

In acidic solutions, the reductions of these molecules were reported to take place at negative electrode potentials (less than – 0.3 V *vs.* Ag|AgCl) and involve protonation, transforming into products. The transformations of these molecules depend on the degree of the protonation, which is highly influenced by solution acidity, the electrode materials and the

concentration of active materials. For example, a two proton–two electron reaction leads to the formation of hydroxyl cyclohexanone (Reaction 6). With the following reductions, the hydroxyl cyclohexanone may be further reduced to cyclohexanediol as the reaction product with an overall contribution of four protons and four electrons as expressed in Reaction 7:

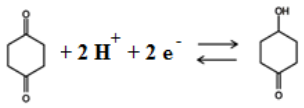

(6)

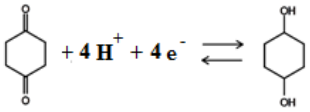

(7)

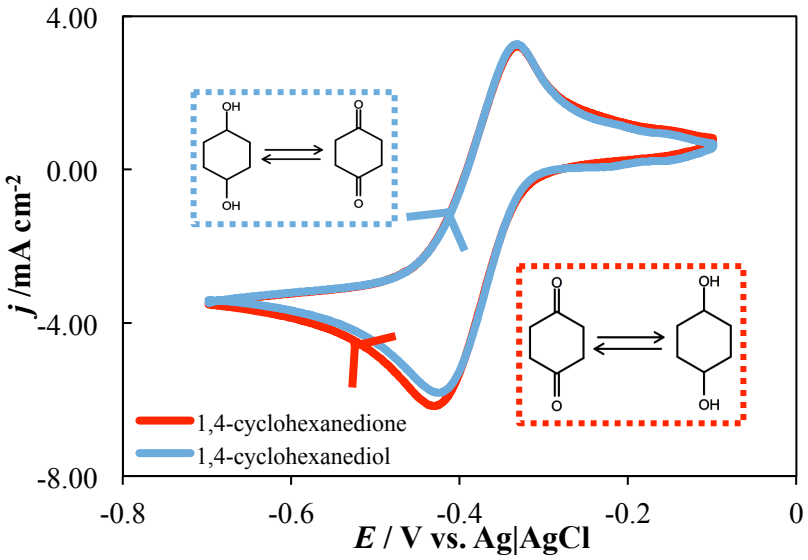

Figure 2

Fig. 2. Cyclic voltammograms for (a) the reduction of 1,4-cyclohexanedione (red curve) and (b) the oxidation of 1,4-cyclohexanediol (blue curve) at a platinum electrode. Electrolyte: 10 mmol dm^{-3} organic molecules in 0.2 mol dm^{-3} sodium chloride solution at pH 2 (adjusted by hydrochloric acid); temperature = 25 ^{o}C; potential sweep rate: 100 mV s^{-1}. The NHE potential scale is obtained by adding 205 mV from Ag|AgCl reference readings.

The above reactions are especially similar to the benzoquinone/hydroquinone reaction, which involve the formation(s) of the hydroxyl functional group(s). In order to better identify the

241 electrochemical reactions involved in these systems, cyclic voltammetry was performed by
242 reducing and oxidizing the starting molecules of cyclohexanedione and cyclohexanediol,
243 respectively, as shown in Figure 2.

244 By using cyclic voltammetry, the active species were reduced or oxidized continuously at the
245 electrodes surfaces over a given potential range (– 0.7 and – 0.1V *vs.* Ag|AgCl), during which
246 a high degree of possible protonation or deprotonation was expected. Since the cyclic
247 voltammogram for the reduction of cyclohexanedione was similar to that for the oxidation of
248 cyclohexanediol, it is believed that the redox reactions between 1,4-cyclohexanedione and
249 1,4-cyclohexanediol are possible, and occur at an electrode potential of *c.a.* – 0.38 V *vs.*
250 Ag|AgCl at pH 2.

251 For the purposes of comparison, a similar approach was carried out for the voltamograms of
252 benzoquinone and hydroquinone (Figure S3) under the same operating conditions. Inspecting
253 both sets of results, we can conclude that the redox reactions of
254 cyclohexanedione/cyclohexanediol are advantageous in terms of their electrode potential and
255 degree of reversibility.

256 Although this work is focused on the protonation process of cyclohexanedione as the
257 negative electrode reaction, two other quasi-reversible reactions are also possible for this
258 molecule at certain active material concentrations and pH values: (1) the oxidation of
259 cyclohexanedione; (2) the formation of hydroxyl-cyclohexene/ dihydroxyl-cyclohexadiene in
260 neutral/less acidic solutions.

261 For the oxidation of cyclohexanedione, the corresponding reactions and mechanisms are still
262 not completely understood [57]. However, since it is an oxidation process, the reactions are
263 believed to be more positive**[you mean occur at more positive potentials?]** than the
264 reduction of the cyclohexanedione. In the case of the reduction processes of these molecules,

the reaction schemes in neutral/ acidic and neutral/ alkaline media are proposed to be as shown in Figure 3a and 3b.

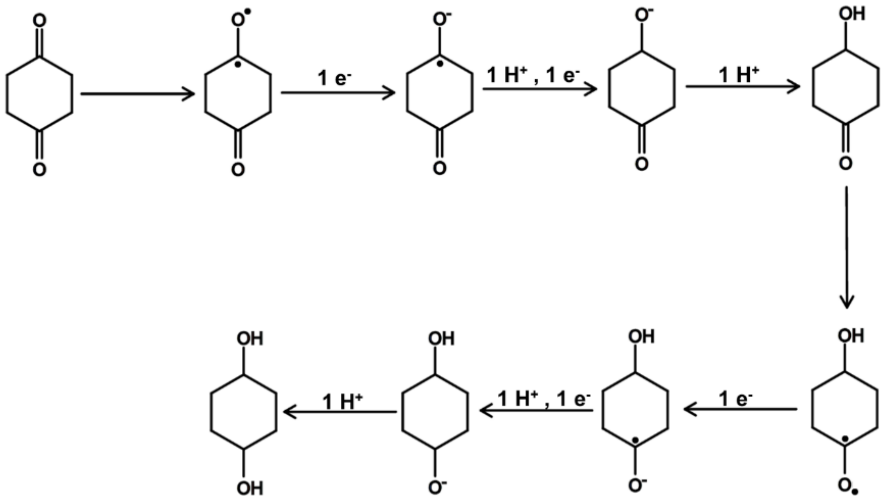

Figure 3a.

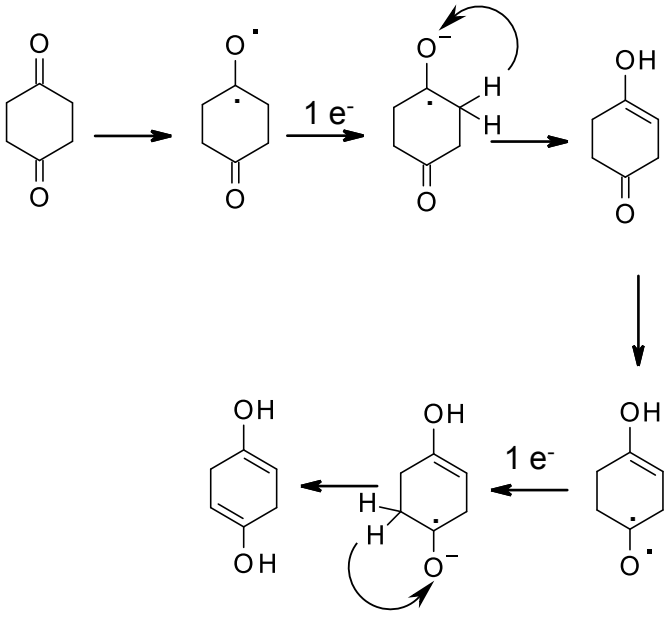

Figure 3b.

Fig. 3. Proposed reaction mechanism routes for (a) neutral/ acidic solution ($[H^+] \geq$ [Organic compound]) and (b) neutral/ alkaline solution ($[H^+] \leq$ [Organic compound]).

For all of these reduction routes, the carbonyl group of the cyclohexanedione involves an electron transfer to form a radical anion in the initial step, which needs to be further reduced or stabilized in different forms in the aqueous electrolytes. Under neutral/ acidic conditions, the initial radical is reduced to hydroxyl-cyclohexanone with the contribution of one external proton and one electron. This is a critical step in this process since it depends heavily on the availability of protons in the electrolytes, although the intermediate formation of semi-quinone (with the addition of one electron) is often considered as a rate-determining step in the similar benzoquinone/ hydroquinone reduction process [58]. Subsequently, the remaining carbonyl group of the hydroxyl cyclohexanone molecule undergoes another two-proton–two-electrons reduction in a similar manner to form the cyclohexanediol molecule.

In the case of alkaline or less acidic solutions, there proton concentration in the electrolytes is too low. The initial radicals tend to be stabilized with the hydrogen atom inside the single bond hydrocarbon ring structure. By receiving an electron, the carbonyl group is replaced by a hydroxyl group and results in a double bond between the two carbon atoms. The reaction products are known as hydroxyl-cyclohexene and dihydroxyl-cyclohexadiene for the one and two-electrons reduction processes, respectively. According to the literature, however, the double bond conjugated with the second carbonyl group is less resonance stabilized compared to that of 1,3-cyclohexanedioe, leading to lower percentage of enol at equilibrium [49]. Furthermore, the second electron reduction process towards the formation of dihydroxyl-cyclohexadiene is not likely since the protons located on α-carbons are less acidic than the methylene proton of 1,3-cyclohexanedione [50] (predicted pKa = 5.26 using Advanced Chemistry Development (ACD/Labs) Software V11.02). For the cases of 1,3-cyclohexanedione, hydroxyl-cyclohexene was mainly observed by gas chromatography-mass spectrometry (GCMS) after prolonged reduction in a parallel-plate flow cell (–20 mA, –3.2 mA cm^{-2} for 100 h) (see Figure S4 in the Supplementary Information). Based on these

297 characteristics, the aforementioned negative electrode reactions will occur more readily at
298 certain values of pH in the following section.

299 **3.1.2. Effect of pH**

300 In Section 3.1.1., cyclic voltamograms of prototypical 1,4-cyclohexanedione were obtained
301 under a wide range of potentials (between – 2.0 and + 1.6 V vs Ag|AgCl), revealing the
302 presence of several reactions. In order to identify the compounds and their electrochemical
303 reactions, it is important to determine the number of protons/electrons involved in each
304 electrode reaction by means of electrochemical methods. Using voltammetric data we can
305 extract the relevant E_0 *vs.* pH plot to evaluate the number of protons in a particular reaction.
306 Based on the linear relationship between E_0 and pH, gradients of – 59 mV pH^{-1}, – 29 mV pH^{-1}
307 and – 0 mV pH^{-1} correspond to the four proton-four electron (or two-proton-two electron),
308 the one-proton-two electrons and zero-proton processes, respectively.

309 Since this work has been focused on the use of cyclohexanedione for the negative electrode
310 reaction in a redox flow battery, a cyclic voltammetry of the three isomeric 1,2-, 1,3- and 1,4-
311 cyclohexanediones was conducted over a wide range of pH values (pH 1 – 11) sweeping the
312 electrode potentials from – 0.1 to – 1.15 V *vs.* Ag|AgCl at 100 mV s^{-1} (Figure 4). Overall, the
313 reduction potentials obtained for 1,2-cyclohexanedione are almost the same as those reported
314 at the aforementioned pH values [50].

315 As shown in Figure 4, only two sets of reactions are observed at negative electrode potentials
316 for each compound under different pH conditions. One reaction was observed at very
317 negative electrode potentials (< – 0.6 V *vs.* Ag|AgCl), with a pair of quasi-reversible peaks.
318 These peaks became smaller or completely masked by hydrogen evolution under acidic pH
319 (less than pH 2) conditions. It should be noted that the cathodic current densities attained at
320 electrode potentials < – 0.4 V *vs.* Ag|AgCl at highly acidic pH 1 solutions (50 mA $cm^{-2} < j <$
321 125 mA cm^{-2}) were significantly higher than those at other pH values (< 25 mA cm^{-2}). Such

large current densities were mainly attributed to the evolution of hydrogen, which tends to take place easily at 0 V vs. SHE (*c.a.* – 0.205 V *vs.* Ag|AgCl) with low hydrogen overpotentials using platinum electrodes. The fluctuations of the recorded electrode potentials were due to the excessive hydrogen bubbles blocking the electrode surfaces, considering that no agitation was applied in the experiments.

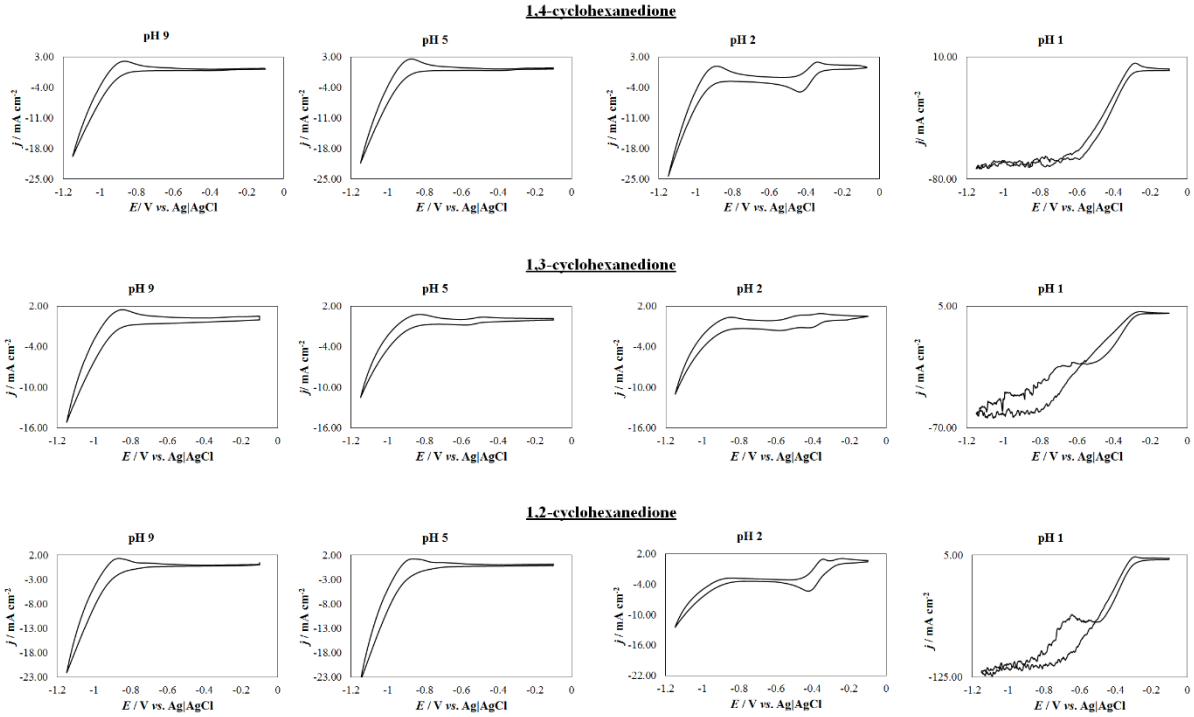

Fig. 4. Effect of pH on cyclic voltammograms for the reduction of 1,2-, 1,3- and 1,4-cyclohexanedione at a platinum electrode. Electrolyte: 10 mmol dm^{-3} cyclohexanedione in 0.2 mol dm^{-3} sodium chloride solution at pH 1, 2, 5 and 9 (adjusted by hydrochloric acid and sodium hydroxide); temperature = 25 ^{o}C; potential sweep rate: 100 mV s^{-1}. The NHE potential scale is obtained by adding 205 mV from Ag|AgCl reference readings.
*The scale of the current density axis is not identical for all voltammograms.

In the case of the 1,2-cyclohexanedione, the most negative peaks no longer appeared at pH 2, in which hydrogen evolution was not yet appreciable according to the cyclic voltammograms.

This means that these reactions can only occur when the proton concentration is sufficiently low compared to the concentration of the active molecules.

The slope of the E_0 *vs*. pH curve shown in Figure S5(a – c) (– 0 mV per pH unit) indicates that protons are not involved in this reaction but they appear to be the formations of hydroxyl-cyclohexene/ dihydroxyl-cyclohexadiene (described in Figure 4(a) and 4(b)) or other relevant radicals depending on the number of electron transfers. In addition to this reaction, the other set of quasi-reversible reactions was observed between – 0.1 and – 0.6 V vs. Ag|AgCl. In comparison to the other negative reaction (< – 0.6 V *vs.* Ag|AgCl), this reaction is at less negative potentials and tends to diminish or disappear in neutral or alkaline solutions (> pH 5). As discussed in Section 3.1.1., this set of reactions has been identified as the redox reactions of cyclohexanedione/hydroxyl cyclohexanone or cyclohexanedione/cyclohexanediol, depending on the availability of protons in the electrolytes.

In such cases, the resulting reactions should involve two protons and two electrons for the formation of hydroxyl cyclohexanone molecules, or involve four protons and four electrons for the formation of the two hydroxyl groups in the cyclohexanediol molecules (see the reaction mechanism route in Figure 3a), which has been confirmed from the slope of the E_0 *vs*. pH plots (– 59 mV per pH) under acidic conditions (Figures S5(a–c)). Furthermore, multi-electron transfers in separate steps were observed at pH 2.5 in the case of 1,3-cyclohexanedione, as shown in Figure S6 in the Supplementary Information.

Despite this, the smaller slope of the E_0 *vs*. pH plot for 1,3-cyclohexanedione (> – 15 mV per pH) indicates that there are fewer protons or more electrons involved in the relevant reaction between pH 2.5 and 5. Considering that the proton concentration is lower than that of the active molecule (i.e. pH 2.5 refers to 0.0032 mol dm^{-3} $[H^+]$), insufficient protons are available

to permit a complete reduction process to form two hydroxyl groups as a cyclohexanediol molecule. The only possibility is that the reaction may be a mixture of several reduction reactions or even involve the reduction products of these processes.

To summarize this section, the 1,3-cyclohexanedione molecule was observed to have a redox electrode potential of up to – 0.6 V *vs.* Ag|AgCl, which is more negative than those for the other isomeric molecules. Additionally, the operating pH (pH 1.5 – 5) is also wider than those for the 1,2- and 1,4-cyclohexanediones (pH 1.5 – 2). This quality is particularly important for prolonged charge-discharge cycling considering that acidity or alkalinity changes are almost inevitable due to the inefficiencies of, and side reactions in batteries. It is important to note that a sufficiently high concentration of protons is necessary for complete conversion during the reduction process, while high acidity tends to promote hydrogen evolution, which impedes the reduction process. This appears to be a major challenge in the way of fully exploiting the high specific capacity (theoretically up to 474 A h Kg^{-1} (2 e^- transfers); 948 A h Kg^{-1} (4 e^- transfers)); hydrogen evolution must be suppressed effectively or very low concentrations of active species must be used at neutral or slightly acidic electrolytes.

For these reasons, we selected 1,3-cyclohexanedione as the preferred molecule to be further investigated in the following sections in relation to its electrochemical behavior during charge and discharge in a flow battery. The redox reaction of this molecule was confirmed to be a mass transport controlled process with an average diffusion coefficient of $< 7.1 \times 10^{-7}$ cm^2 s^{-1} obtained from the Randles-Sevcik and Levich equations as described in the Supplementary Information (see 'Effect of Scan Rate' and 'Effect of Rotating Speed').

3.2. Galvanostatic Half-Cell Charge-Discharge Experiments

In Section 3.1., the electrochemical characterization of the redox reactions of the 1,3-cyclohexanedione molecules were investigated using voltammetric techniques. Experimental

results show that the redox reactions are mass transport controlled and are reversible at relatively negative electrode potential (*c.a.* – 0.6 V *vs.* Ag|AgCl). In order to justify the use of this reaction for redox flow battery applications, half-cell charge-discharge experiments were carried out in a divided parallel-plate flow cell. The electrolyte composition was 0.2 M 1,3-cyclohexanedione in 0.2 M sodium chloride at pH 3.5. The charge-discharge process was performed under a 30 min charge – 30 min discharge regime at 3.2 mA cm^{-2} (20 mA) for 100 cycles (Figures 5a, complete charge-discharge cycles are available in Figure S7 in Supplementary Information).

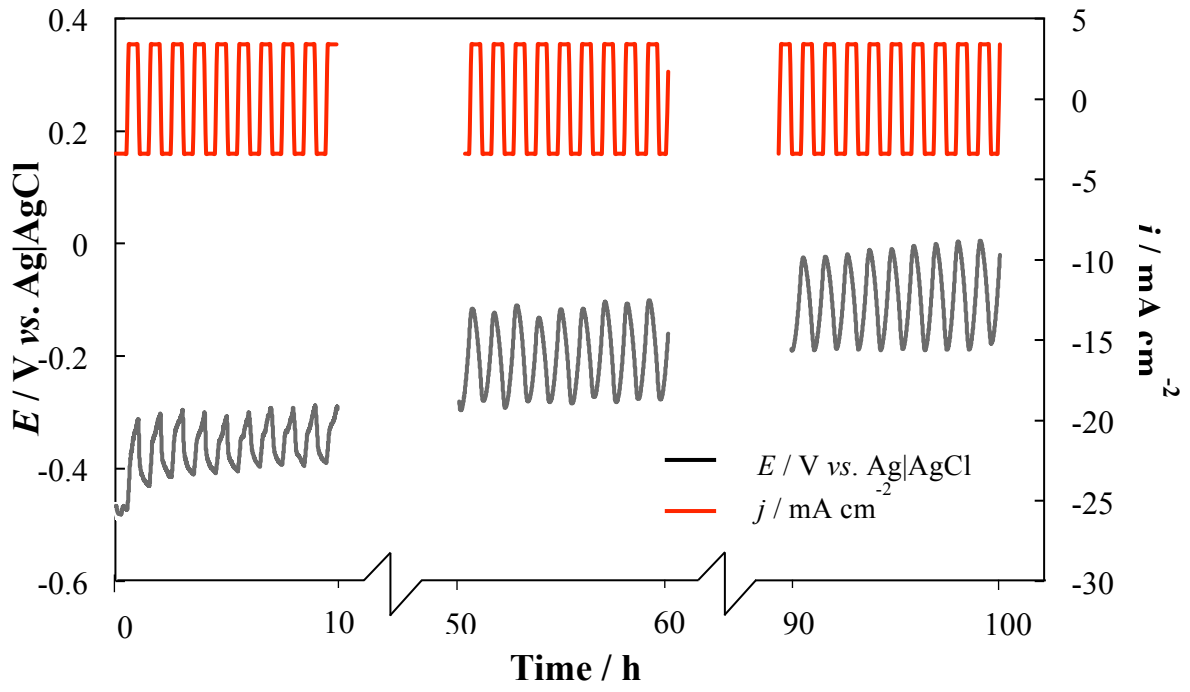

Figure 5a

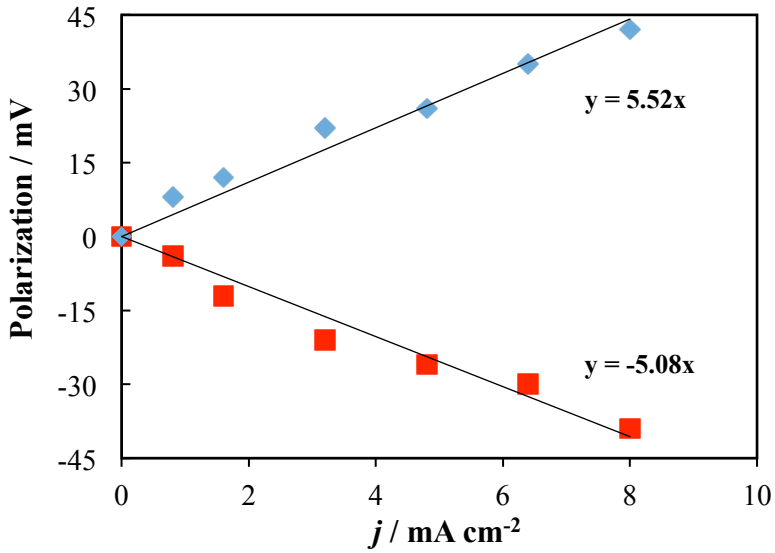

390

391 **Figure 5b**

392

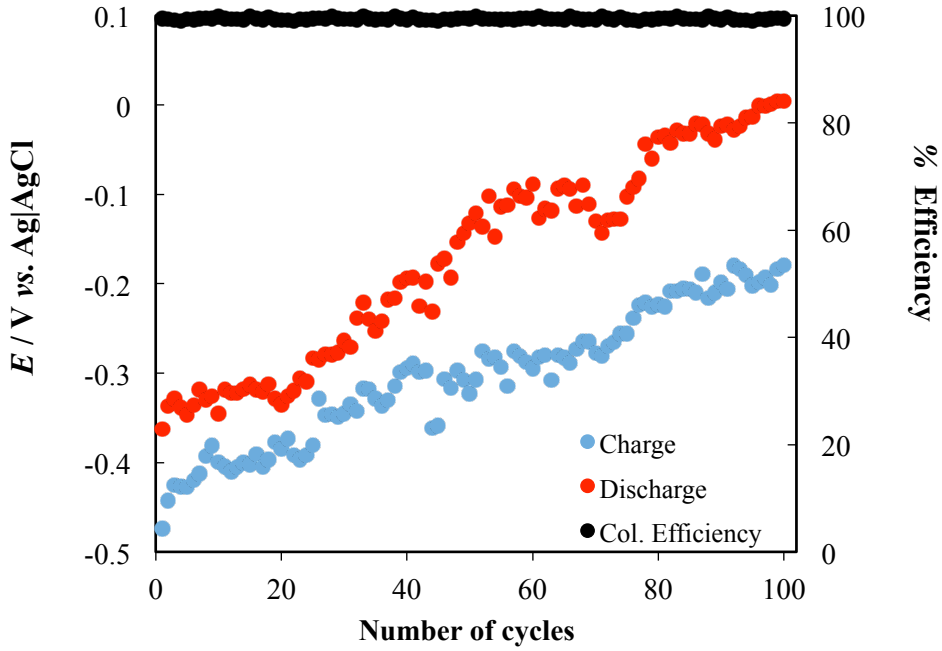

393

394 **Figure 5c**

Fig. 5. Half-cell performance of the cyclohexanedione reaction in a parallel plate flow cell: (a) the electrode potential *vs.* time response using a 30 min charge – 30 min discharge regime at 20 mA (3.2 mA cm^{-2}) for 100 cycles; (b) polarization performances at negative and positive current densities between 0 and 8 mA cm^{-2}; (c) the system efficiencies and charge-discharge potentials (at 20 mA for 100 cycles). Electrolyte: 0.2 mol dm^{-3} 1,3-cyclohexanedione + 0.2 mol dm^{-3} sodium chloride. Room temperature.

395

Prior to this test, the open-circuit potential was *c.a.* – 0.42 V *vs.* Ag|AgCl, which is comparable to the formal electrode potential, E_0, obtained in the voltammetric studies. Despite the flowing electrolyte **[did you state the flow rate?]**, the applied current density (3.2 mA cm^{-2}) was relatively high, and comparable to the peak current densities obtained (2 – 4 mA cm^{-2}) in the cyclic voltammetry study (Figure 4). Since the concentration of cyclohexanediol was much lower than that of cyclohexanedione, mass transport of cyclohexanediol to the electrode surface was not sufficiently fast to maintain a flat voltage profile, especially without the use of a high-surface-area/porous electrode. During the initial cycles, the reduction (charge) and oxidation (discharge) potentials were *c.a.* – 0.47 and *c.a.* – 0.37 V *vs.* Ag|AgCl, respectively, while the half-cell coulombic efficiencies were as high as 99 %.

The half-cell coulombic efficiencies were obtained using Equation (5). At different current densities, the corresponding polarizations in the charge and discharge processes are shown in Figure 5b, in which the area resistance was calculated as 5.3 Ω cm^{-2} at 25 ^{o}C. This value can be reduced significantly by using high-surface-area electrodes as in conventional systems. After subsequent cycles, however, the electrode potentials had a tendency to increase towards more positive values (to more acidic due to the evolution of oxygen in the counter reaction). For instance, the reduction (charge) and oxidation (discharge) potentials shifted to around – 0.20 and *c.a.* + 0.0 V *vs.* Ag|AgCl, respectively, in the 100th cycle (Figure 5c).

This tendency could be attributed to changes in the electrolyte caused by various factors, such as air oxidation, pH variations, electrolyte degradation and cross-mixing with the species in the positive electrolyte. The increasing potential is attributed to the mixed potentials of the cyclohexanedione/cyclohexanediol reaction and the possible side reactions. As suggested from the cyclic voltammetry (Figure 1), the oxidation of cyclohexaneione was the main

source of side reactions rather than oxygen evolution, which was observed to have poor reversibility and an electrode potential as high as +1.1 V *vs.* Ag|AgCl.

At the end of the cycling, the potential drop between the charge and discharge processes increased to around 370 mV compared to 100 mV in the initial cycles. In all charge-discharge cycles, the half-cell coulombic efficiencies were observed to remain at nearly 99 % (Figure 5c), which suggests that the redox reactions of the 1,3-cyclohexanedione are sufficiently reversible to be used as the negative electrode species in organic flow batteries. Considering that up to four electrons can be involved in the reduction process, the use of the redox processes in this group of organic molecules can be coupled with a number of commercially available electropositive organic redox couples (i.e. 1,2-hydroquinone-disulfonic acid (+0.85 V *vs.* SHE), 4-hydroxyl-TEMPO (+0.80 V *vs.* SHE), potentially yielding an aqueous all-organic redox flow battery with a cell voltage of more than 1.0 V. This represents a new research direction for cost-effective, large-scale energy storage.

Conclusions

In this work, the electrochemical behaviour of the three isomeric 1,2-, 1,3- and 1,4-cyclohexanediones was studied using voltammetric techniques under a wide range of pH (pH 1 – 11). Experimental results show that the reduction of cyclohexanedione is a quasi-reversible reaction requiring catalysts (e.g. platinum). In acidic media (< pH 3), these reactions has been confirmed to be proton-coupled electron transfer process at negative electrode potentials of < – 0.3 V *vs.* Ag|AgCl.

Observations from the voltammetric study and the *E vs.* pH diagrams appear to be consistent with the proposed reduction reaction schemes in neutral/acidic (formation of hydroxyl cyclohexanone/cyclohexanediol) and neutral/alkaline (formation of hydroxyl-cyclohexene/dihydroxyl-cyclohexadiene) media electrolytes. For both reduction routes, the

carbonyl group of the cyclohexanedione involves an electron transfer to form a radical anion in the initial step, which needs to be further reduced or stabilized in different forms in the aqueous electrolyte. Under neutral/ acidic conditions, the initial radical is reduced to hydroxyl-cyclohexanone with the contribution of one external proton and one electron. Subsequently, the remaining carbonyl group of the hydroxyl cyclohexanone molecule undergoes another two-proton–two-electron reduction in a similar manner to form the cyclohexanediol molecule.

In the case of alkaline or less acidic solutions, the aforementioned initial radicals tend to be stabilized with the hydrogen atom inside the single bond hydrocarbon ring structure due to the low proton concentrations in the electrolytes. By receiving an electron, the carbonyl group is replaced by a hydroxyl group, which results in a double bond between the two carbon atoms. The reaction products are hydroxyl-cyclohexene and dihydroxyl-cyclohexadiene for the one and two-electrons reduction processes, respectively.

Among the three isomeric molecules, 1,3-cyclohexanedione was observed to possess the most negative electrode potentials (up to – 0.6 V *vs.* Ag|AgCl) and the widest pH operating range (pH 1 – 5) for reversible electrochemical behaviour. The redox reaction of the resulting 1,3-cyclohexanedione was confirmed to be a mass transport controlled process with an average diffusion coefficient of $< 7.1 \times 10^{-7}$ cm^2 s^{-1} obtained from the Randles-Sevcik and Levich equations.

Despite the high half-cell coulombic efficiencies (*c.a.* 99 %) of the parallel plate redox flow battery employing 1,3-cyclohexanedione, the reduction (charge) and oxidation (discharge) potentials tended to shift more positive values after repeated cycling, possibly due to the mixed potentials of the cyclohexanedione/cyclohexanediol reaction and the possible side reactions (oxidation of cyclohexanedione).

Further investigations should focus on the use of several functional groups (i.e. OH–, CH_3–, NH_2–) to obtain more negative electrode potentials while inhibiting hydrogen evolution in proton-rich acidic electrolyte. Additionally, the use of high-surface-area electrodes with low platinum loadings could reduce the overpotentials at high current densities.

Acknowledgements

AAS acknowledges financial support from the EPSRC (Grant No. EP/P012620/1).

References

[1] The EU Emissions Trading System (EUETS), Climate Action, http://ec.europa.eu/clima/policies/ets/index_en.htm

[2] Energy from renewable sources, Eurostat, http://ec.europa.eu/eurostat/statistics-explained/index.php/Energy_from_renewable_sources (accessed on 05th December, 2016)

[3] M. Skyllas-Kazacos, M.H. Chakrabarti, S.A. Hajimolana, F.S. Mjalli, M. Saleem, Progress in Flow Battery Research and Development, ***J. Electrochem. Soc.***, 2011, 158, R55-R79.

[4] J. Noack, N. Roznyatovskaya, T. Herr, P. Fischer, The Chemistry of Redox-Flow Batteries, ***Angew. Chem Int Ed.***, 2015, 54, 9776 – 9809.

[5] C. Ponce de Leon, A. Frias-Ferrer, J. Gonzalez-Garcia, D.A. Szanto, F.C. Walsh, Redox flow cells for energy conversion, ***J. Power Sources***, 2006, 160, 716 – 732.

[6] P. Leung, X. Li, C. Ponce de Leon, L. Berlouis, C.T.J. Low, F.C. Walsh, Progress in redox flow batteries, remaining challenges and their applications in energy storage, ***RSC Adv.***, 2012, 2, 10125-10156.

[7] T. Sun, Z-J. Li, H-G. Wang, D. Bao, F-L. Meng, X-B. Zhang, A Biodegradable Polydopamine-Derived Electrode Material for High-Capacity and Long-Life Lithium-Ion and Sodium-Ion Batteries, ***Angew. Chem. Int. Ed.***, 2016, 55, 10662 – 10666.

[8] H. Zhong, J. Wang, X-B. Zhang, In Situ Activating Ubiquitous Rust towards Low-Cost, Efficient, Free-Standing, and Recoverable Oxygen Evolution Electrodes, ***Angew. Chem. Int. Ed.***, 2016, 55, 9937 – 9941.

[9] H-G. Wang, S. Yuan, D-L. Ma, X-L. Huang, F-L. Meng, X-B. Zhang, Tailored Aromatic Carbonyl Derivative Polyimides for High-Power and Long-Cycle Sodium-Organic Batteries, ***Adv. Energy Mater***., 2014, 4, 1401651.

[10] F. Meng, H. Zhong, D. Bao, J. Yan, X. Zhang, In Situ Coupling of Strung Co_4N and Interwined N-C Fibers towards Free-Standing Bifunctional Cathode for Robust, Efficient, and Flexible Zn-Air Batteries, ***J. Am. Chem. Soc.***, 2016, 138, 10226 – 10231.

[11] Grid Energy Storage, U.S. Department of Energy, 2013. http://energy.gov/oe/downloads/grid-energy-storage-december-2013

[12] M.R. Mohamed, P.K. Leung, M.H. Sulaiman, Performance characterization of a vanadium redox flow battery at different operating parameters under a standardized test-bed system, ***Applied Energy***, 2015, 137, 402-412.

[13] P.K. Leung, C. Ponce de Leon, C.T.J. Low, A.A. Shah, F.C. Walsh, Characterization of a zinc-cerium flow battery, ***J. Power Sources***, 2011, 196, 5174 – 5185.

[14] P.K. Leung, M.R. Mohamed, A.A. Shah, Q. Xu, M. B. Conde-Duran, A mixed acid based vanadium-cerium redox flow battery with a zero-gap serpentine architecture***, J. Power Sources***, 2015, 274, 651 – 658

[15] P. Leung, J. Palma, E. Garcia-Quismondo, L. Sanz, M.R. Mohamed, Evaluation of electrode materials for all-copper hybrid flow batteries, ***J. Power Sources***, 2016, 310, 1 – 11.

[16] Y.K. Zeng, T.S. Zhao, L. An, X.L. Zhou, L. Wei, A comparative study of all-vanadium and iron-chromium redox flow batteries for large-scale energy storage, ***J. Power Sources***, 2015, 300, 438 – 443.

[17] L. Joerissen, J. Garche, Ch. Fabjan, G. Tomazic, Possible use of vanadium redox-flow batteries for energy storage in small grids and stand-alone photovoltaic systems, ***J. Power Sources***, 127, 2004, 98 -104.

[18] Presentation of B. Huskinson et al. at Princeton Uni. 20/10/2014, http://acee.princeton.edu/wp-content/uploads/Aziz-Princeton-Slides-2014-10-20-Organic-Based-Aqueous-Flow-Batteries-for-Massive-Electrical-Energy-Storage.pdf (accessed on 05th December, 2016)

[19] B. Huskinson, M.P. Marshaw, C. Suh, M.R. Gerhardt, C.J. Galvin, X. Chen, A. Aspuru-Guzik, R. G. Gordon, M. J. Aziz, A metal-free organic-inorganic aqueous flow battery, ***Nature***, 2014, 505, 195 – 198.

[20] Presentation of F. Brushett at 2nd Annual MRES Conference, Northeastern Uni. 18/11/2014, Non-aqueous redox flow batteries: Challenges & Opportunities, http://nuweb9.neu.edu/mres/wp-content/uploads/2014/11/Fikile-Brushett-presentation.pdf

[21] F. R. Brushett, J. T. Vaughey, A.N. Jansen, An All-Organic Non-aqueous Lithium-Ion Redox Flow Battery, ***Adv. Energy Mater.***, 2012, 2, 1390 – 1396.

[22] E.V. Carino, C.E. Diesendruck, J. S. Moore, L.A. Curtiss, R.S. Assary, F.R. Brushett, BF3-promoted electrochemical properties of quinoxaline in propylene carbonate, ***RSC Advances***, 2015, 5, 18822 – 18831.

[23] J.D. Milshtein, L. Su, C. Liou, A.F. Badel, F.R. Brushett, Voltammetry study of quinoxaline in aqueous electrolytes, ***Electrochim. Acta***, 2015, 180, 695 – 704.

[24] Z. Li, S. Li, S. Liu, K. Huang, D. Fang, F. Wang, S. Peng, Electrochemical Properties of an all-organic redox flow battery using 2,2,6,6-Tetramethyl-Piperidinyloxy and N-Methylphalimide, ***Electrochem. Solid-State Lett***., 2011, 14, A171 – A173.

[25] K. Gong, Q. Fang, S. Gu, S. F. Y. Li, Y. Yan, Nonaqueous Redox-Flow

Batteries: Organic Solvents, Supporting Electrolytes, and Redox Pairs, ***Energy Environ. Sci.***, 2015, 8, 3515 – 3530.

[26] Alibaba.com, http://www.alibaba.com/trade/search?fsb=y&IndexArea=product_en&CatId=&SearchText=Propylene+carbonate (accessed on 05th December, 2016)

[27] European Environmental Agency, Agricultural, Industrial and Household water prices in late 1990s, http://www.eea.europa.eu/data-and-maps/figures/agricultural-industrial-and-household-water-prices-in-late-1990s (accessed on 05th December, 2016)

[28] X. Wang, M. Li, Y. Wang, B. Chen, Y. Zhu, Y. Wu, A Zn-NiO rechargeable battery with long lifespan and high energy density, ***J. Mater. Chem.A***., 2015, 3, 8280 – 8283.

[29] B. Zhang Y. Liu, X. Wu, Y. Yang, Z. Chang, Z. Wen, Y. Wu, An aqueous rechargeable battery based on zinc anode and $Na_{0.95}MnO_2$, ***Chem. Commun***., 2014, 50, 1209 – 1211.

[30] X. Wang, F. Wang, L. Wang, M. Li, Y. Wang, B. Chen, Y. Zhu, L. Fu, L. Zha, L. Zhang, Y. Wu, W. Huang, An Aqueous Rechargeable Zn//Co_3O_4 Battery with High Energy Density and Good Cycling Behaviour, ***Adv. Mater.***, 2016, 28, 4904 – 4911.

[31] P.K. Leung, Q. Xu, T.S. Zhao, High-potential zinc-lead dioxide rechargeable cells, ***Electrochim. Acta***, 2012, 79, 117 – 125.

[32] Y. Ding, Y. Li, G. Yu, Exploring Bio-inspired Quinone-Based Organic Redox Flow Batteries: A Combined Experimental and Computational Study, ***Chem***, 2016, 1, 790 – 801.

[33] B. Yang, L. Hoober-Burkhardt, F. Wang, G.K. Surya Prakash, S.R. Narayanan, An Inexpensive Aqueous Flow Battery for Large-Scale Electrical Energy Storage Based on Water-Soluble Organic Redox Couples, ***J. Electrochem. Soc.***, 2014, 161, A1371– A1380.

[34] K. Lin, Q. Chen, M.R. Gerhardt, L. Tong, S. B. Kim, L. Eisenach, A. W. Valle, D. Hardee, R.G. Gordon, M.J. Aziz, M. P. Marshak, Alkaline quinone flow battery, ***Science***, 2015, 349, 1529 – 1532.

[35] K. Lin, R. Gomez-Bombarelli, E.S. Beh, L. Tong, Q. Chen, A. Valle, A. Aspuru-Guzik, M.J. Aziz, R.G. Gordon, A redox- flow battery with an alloxazine-based organic electrolyte, ***Nature Energy***, 2016, 1, 16102.

[36] E.S. Beh, D.D. Porcellinis, R.L. Gracia, K.T. Xia, R.G. Gordon, M.J. Aziz, A Neutral pH Aqueous Organic/Organometallic Redox Flow Battery with Extremely High Capacity Retention, ***ACS Energy Letters***, 2017, 2, 639 – 644.

[37] T. Liu, X. Wei, Z. Nie, V. Sprenkle, W. Wang, A Total Organic Aqueous Redox Flow Battery Employing a Low Cost and Sustainable Methyl Viologen,anolyte and 4-HO-TEMPO catholyte, ***Adv. Energy. Mat.***, 2016, 6, 1501449.

[38] J. Winsberg, T. Hagemann, T. Janoschka, M. D. Hager, U.S. Schubert, Redox-Flow Batteries: From Metals to Organic Redox-Active Materials, ***Angew. Chem.***

Int. Ed., 2016, 56, 686 – 711.

[39] J.A. Kowalski, L. Su, J.D. Milshtein, F.R. Brushett, Recent advances in molecular engineering of redox active organic molecules for nonaqueous flow batteries, ***Curr Opin Chem Eng***, 2016, 13, 45 – 52.

[40] P.K. Leung, T. Martin, A.A. Shah, M.R. Mohamed, M.A. Anderson, J. Palma, Membrane-less hybrid flow battery based on low-cost elements, ***J. Power Sources***, 2017, 341, 36 – 45.

[41] P.K. Leung, T. Martin, A.A. Shah, M.A. Anderson, J. Palma, Membrane-less organic-inorganic aqueous flow batteries with improved cell potential, ***Chem. Commun***., 2016, 52, 14270 – 14273.

[42] L. Soloveichik, Electrochemical Energy Conversion and Storage, ***US Patent*** *8,338,055 B2*, 25/12/2012.

[43] S. Er, C. Suh, M.P. Marshak, A. Aspuru-Guzik, Computational design of molecules for an all-quinone redox flow battery, ***Chem. Sci.***, 2015, 6, 885 – 893.

[44] L. N. Monsalve, P. Cerrutti, M. A. Galvagno, A. Baldessari, . Rhodotorula minuta-mediated bioreduction of 1,2-diketones ***Biocat. Biotrans.*** 2010, 28(2), 137-143.

[45] K. Leijondahl, A.-B. L. Fransson, J. E. Baeckvall, Efficient Ruthenium-Catalyzed Transfer Hydrogenation/Hydrogenation of 1,3-Cycloalkanediones to 1,3-Cycloalkanediols Using Microwave Heating ***J. Org. Chem.***, 2006, 71(22), 8622-8625

[46] J. Wang, K. Okumura, S. Jaenicke, G.-K. Chuah, Post-synthesized zirconium-containing Beta zeolite in Meerwein-Ponndorf-Verley reduction: Pros and cons ***Appl. Cat. A: Gen.*** 2015, 493, 112-120.

[47] M. R. Montoya, M.A. Zon, J.M.R. Mellado, Investigation of the reduction of 1, 2-cyclohexanedione and methylglyoxal on mercury electrodes under pure kinetic conditions by linear-sweep voltammetry, ***J. Electroanal. Chem.***, 1993, 353, 217 – 224.

[48] M.A. Zon, J.M.R. Mellado, Study of the electrochemical reduction of unhydrated 1,2-cyclohexanedione on mercury electrodes, ***J. Electroanal. Chem***., 1992, 338, 229 – 238.

[49] J.P. Segretario, N. Sleszynski, P. Zuman, Polarographic reduction of aldehydes and ketones: Part XXVIII. 1,2-cyclohexanedione, ***J. Electroanal. Chem.***, 1986, 214, 259 – 273.

[50] N.N. Niufar, Fiona L. Haycock, J.L. Wesemann, J.A. MacStay, V. L. Heasley, P. Kovacic, Reduction Potentials of Conjugated Aliphatic Ketones, Oximes, and Imines: Correlation with Structure and Bioactivity, ***Revista de la Sociedad Quimica de Mexico***, 2002, 46, 307 – 312.

[51] S. K. Sharma, G. Wadhvani, P.S. Verma, I.K. Sharma, Synthesis of 3-Hydroxy cyclohexanone by Electrochemical and Microbial techniques, ***Int. J. Chem Tech***, 2014, 6, 1462 – 1469.

[52] T. Luczak, R. Holze, M- Beltowska-Brzezinska, The oxidation of cyclic diols on a gold electrode: Structure-reactivity reactions, ***Electronalaysis***, 1994, 6, 773 –

778.

[53] L. Wei, T.S. Zhao, G. Zhao, L. Zeng, X.L. Zhou, Y.K. Zeng, Titanium Carbide Nanoparticle-Decorated Electrode Enables Significant Enhancement in Performance of All-Vandium Redox Flow Batteries, ***Energy Technology***, 2016, 4, 990 – 996.

[54] L. Wei, T.S. Zhao, G. Zhao, L. An, L. Zeng, A high-performance carbon nanoparticle-decorated graphite felt electrode for vanadium redox flow batteries, ***Applied Energy***, 2016, 176, 74 – 79.

[55] C. Zhang, T.S. Zhao, Q. Xu, L. An, G. Zhao, Effects of operating temperature on the performance of vanadium redox flow batteries, ***Applied Energy***, 2015, 155, 349 – 353.

[56] X.L. Zhou, T.S. Zhao, L. An, Y.K. Zeng, X.B. Zhu, Performance of a vanadium redox flow battery with a VANADion membrane, ***Applied Energy***, 2016, 180. 353 – 359.

[57] S. Torii, K. Uneyama, T. Onishi, Y. Fujita, K. Michihiro, I. Kurashiki, T. Nishida, 1,3-cyclohexanedione derivatives, ***US Patent*** *4,336,202*, 22/06/1980.

[58] Chapter 20 Electrochemical Reduction and Oxidation, Electro Chemistry, edited by B.K. Sharma, GOEL Publishing House, 5th edition, 1997, Pg. E-250.

Electronic Supplementary Information

Cyclohexanedione as the negative electrode reaction for organic redox flow batteries

P. Leung[a,b,†], T. Martin[a], M. Liras[a], A.M. Berenguer[a], R. Marcillia[a], A. Shah [c], M.A. Anderson[a,d], J. Palma[a]

a. IMDEA Energy Institute, Mostoles, Spain.

b. Department of Materials, University of Oxford, Oxford, United Kingdom.

c. School of Engineering, University of Warwick, Coventry, United Kingdom.

d. Environmental Chemistry & Technology Program, University of Wisconsin-Madison, United States.

† puiki.leung@materials.ox.ac.uk;

Effect of Scan Rate

The main text of this article shows that the 1,3-cyclohexanedione molecules displayed the most negative electrode potentials and the widest working pH range of all isomeric compounds studied. Figure S1a shows the effect of the potential sweep rate on the cyclic voltammetry of the 1,3-cyclohexanedione reaction on a platinum electrode in a solution containing 10 mmol dm^{-3} cyclohexanedione and 0.2 mol dm^{-3} sodium chloride at pH 3.5.

By increasing the potential sweep rate, the cathodic and anodic peak potentials shifted towards more negative and more positive values, respectively. This results in larger peak separations between the reduction and oxidation processes. For instance, the peak separation increased from 30 mV at 9 mV s^{-1} to 62 mV at 100 mV s^{-1}. Meanwhile, the cathodic and anodic peak current densities increased linearly with the square root of the potential sweep rates, as indicated by the Randles-Sevick relationship (Figure S1b). When $T = 25$ ºC:

$$I_p = 268600\, n^{\frac{3}{2}}\, A\, D^{\frac{1}{2}}\, C\, v^{\frac{1}{2}} \quad (7)$$

where I_P is the current in A, n is the number of electrons, F is the Faraday constant in C mol^{-1}, A is the electrode area in cm^2, D is the diffusion coefficient in $cm^2\ s^{-1}$, C is the electrolyte

concentration in mol cm^{-3}, v is the scan rate in V s^{-1} and R is the molar gas constant (8.3145 J mol^{-1} K^{-1}).

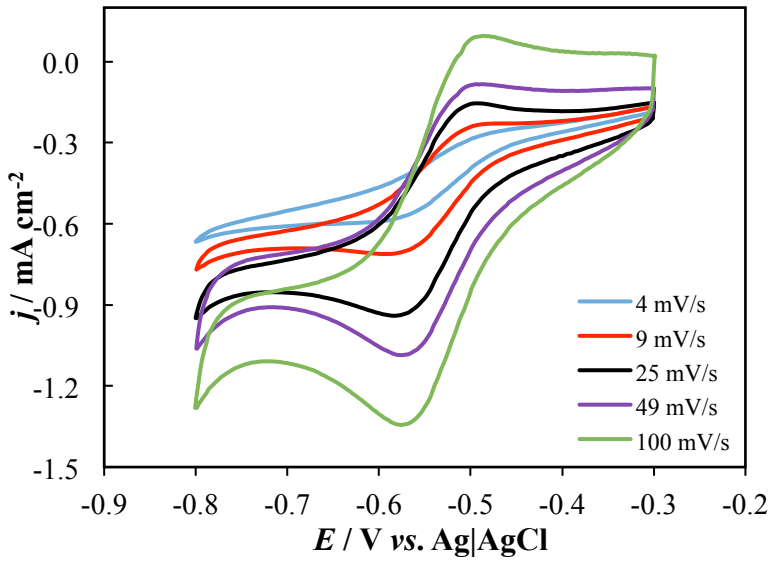

Figure S1a

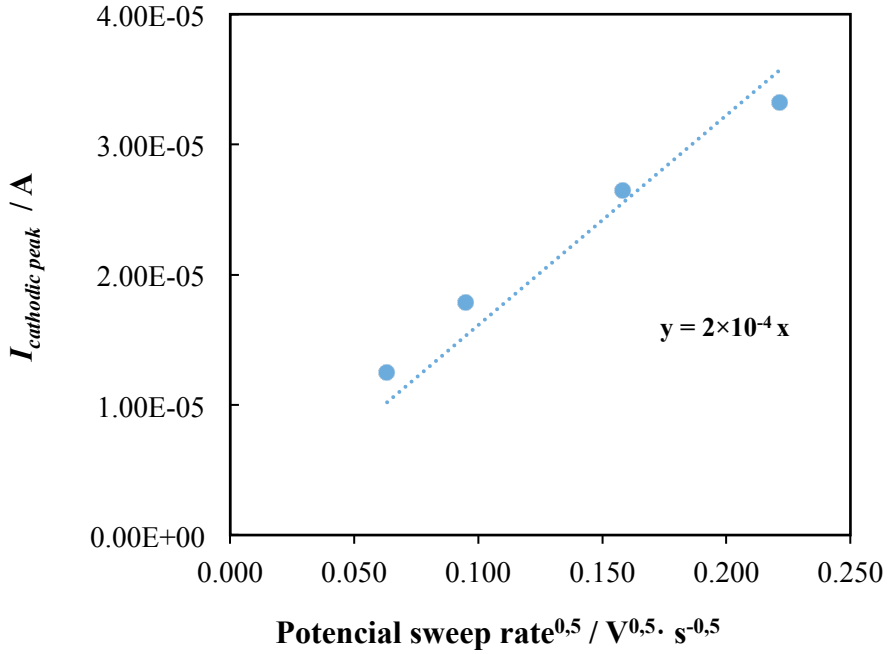

Figure S1b

Fig. S1. The effect of the potential sweep rate on the reduction of 10 mmol dm^{-3} cyclohexanedione in 0.2 mol dm^{-3} sodium chloride solution (pH 3.5) using a platinum disk electrode. (a) Cyclic voltammogram and (b) Randles-Sevcik plot. The potential sweep rates were 4, 9 , 25, 49, 100 mV s^{-1}.

These results indicate that the redox reactions of cyclohexanedione are diffusion limited. Using the value of the gradient from the plot for the reduction process, the diffusion coefficient of 1,3-cyclohexanedione was estimated to be $\geq 9.0\times10^{-7}$ cm^2 s^{-1} at 25 ^oC. The calculated value agrees with previous measurements related to the reduction process of the 1, 2-cyclohexanedione molecules using mercury electrodes at pH 2 (2.3×10^{-6} cm^2 s^{-1}) [1, 2]. However, the value is still slightly lower than that of the quinone molecules (5.0×10^{-6} cm^2 s^{-1}) in aqueous solutions (25 ^oC). The differences can be attributed to the solvation and the interaction of the ionic groups with water through hydrogen bonding [1] or the complexations of organic species in chloride media.

Effect of Rotating Speed

In order to study the influence of mass transport, linear sweep voltammetry of the reduction of the 1,3- cyclohexanedione was performed on a platinum rotating disk electrode at various speeds: 100, 225, 400, 625, 900, 1600 and 2500 rpm. The electrolyte compositions were the same as those used in the previous section.

As shown in Figure S2a, the reduction of 1, 3-cyclohexanedione was observed at a similar potential (– 0.4 to – 0.7 V *vs.* Ag|AgCl) as in the relevant voltammogram in Section 3.1.1., accompanied by the other reduction reactions at more negative electrode potentials (more negative than –0.7 V *vs.* Ag|AgCl). The limiting current density for each rotating speed was measured at the mid-point of the hill at *c.a.* – 0.6 V *vs.* Ag|AgCl regarding the reduction reaction of the 1, 3-cyclohexanedione. The liming current density was observed to increase linearly with the square root of the rotation rate, following the Levich equation (Figure S2b):

$$I_L = 0.620\, n\, F\, A\, D^{\frac{2}{3}}\, \omega^{\frac{1}{2}}\, v^{\frac{-1}{6}}\, C \qquad (8)$$

where I_L is the Levich current in A and F is the Faraday constant in C mol^{-1} (other symbols defined as in Equation (7)).

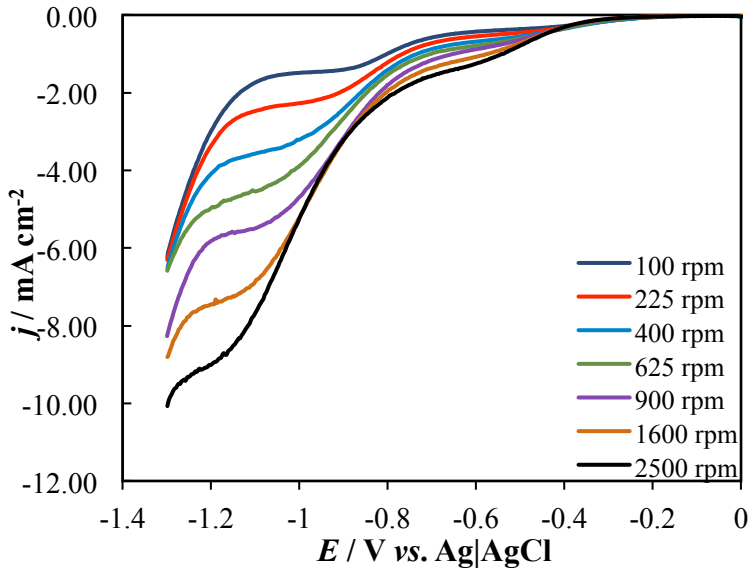

551

552 **Figure S2a**

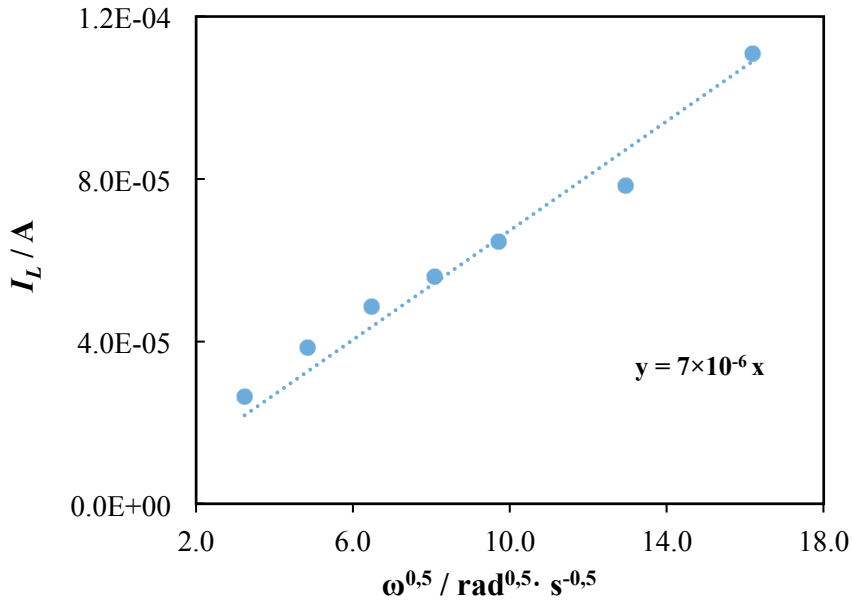

553

554 **Figure S2b**

Fig. S2. The effect of the rotating speed on the reduction of 10 mmol dm^{-3} cyclohexanedione in 0.2 mol dm^{-3} sodium chloride solution (pH 3.5) using a platinum rotating disk electrode. (a) Cyclic voltammogram and (b) Levich plot. The rotating speeds were 100, 225, 400, 625, 900, 1600, 2500 rpm.

555

This behavior indicated that the reduction process of 1,3-cyclohexanedione (10 mmol dm^{-3}) was under complete mass transport control. Using the gradient of this plot, a diffusion coefficient of 7.1×10^{-7} cm^2 s^{-1} was calculated according to the number of electron involved. The resulting value is consistent with the result obtained from the Randles-Sevcik equation (9.0×10^{-7} cm^2 s^{-1}), with less than 25 % deviation.

Proposed negative reaction	Molecular Weight / g mol^{-1}	Specific capacity / A h Kg^{-1}	Electrode potential / V *vs.* NHE	No. of electron - transfer	Supporting electrolytes	Reaction routes	Year
9,10-anthraquinone-2 sulfonic acid	328	161.9 (2 e^-)	+ 0.09 V	2	1 M H_2SO_4 (acidic)	Protonation/ Deprotonation	2014 [3]
Polymer-based viologen	Nil	Nil	– 0.30 V	1	2 M NaCl (neutral)	Radical	2015 [4]
Quinoxaline	130.15	412 (if 2 e^-)	– 0.50 V	Nil	0.2 M KOH (alkaline)	Nil	2015 [5]
2,6-dihydroxyl-anthraquinone	> 200	< 268 (2 e^-)	– 0.65 V	2	1 M KOH (alkaline)	Radical	2015 [6]
Alloxazine	> 200	< 268 (if 2 e^-)	– 0.62V	Nil	KOH, pH 14 (alkaline)	Nil	2016 [7]
Cyclohexanedione	112.12	948 (4 e^-) 474 (2 e^-)	– 0.40 V	2 to 4	0.2 M NaCl (neutral)	Protonation/ Deprotonation	2017 [This work]

Table S1. Proposed negative electrode reactions used in aqueous electrolytes prior to this work.

	1,4-cyclohexanedione	1,3-cyclohexanedione	1,2-cyclohexanedione
Total Peaks	67	47	71
Top Peak / m/z	56	42	112
2nd highest Peak / m/z	112	84	55
3rd highest Peak / m/z	27	55	56
Probability / %	> 85	> 80	> 80

Table S2. Summary of the gas chromatography-mass spectrometry of 1,4-,1,3- and 1,2-cyclohexaneione.

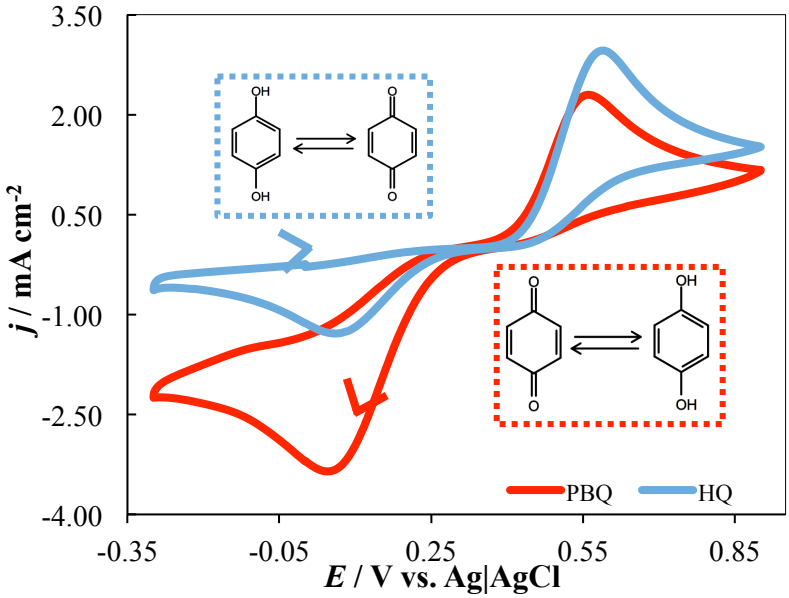

Figure S3

Fig. S3. Cyclic voltammograms for (a) the reduction of benzoquinone (red curve) and (b) the oxidation of hydroquinone (blue curve) at a platinum electrode. Electrolyte: 10 mmol dm^{-3} organic molecules in 0.2 mol dm^{-3} sodium chloride solution at pH 2 (adjusted by hydrochloric acid); temperature = 25 ^{o}C; potential sweep rate: 100 mV s^{-1}.

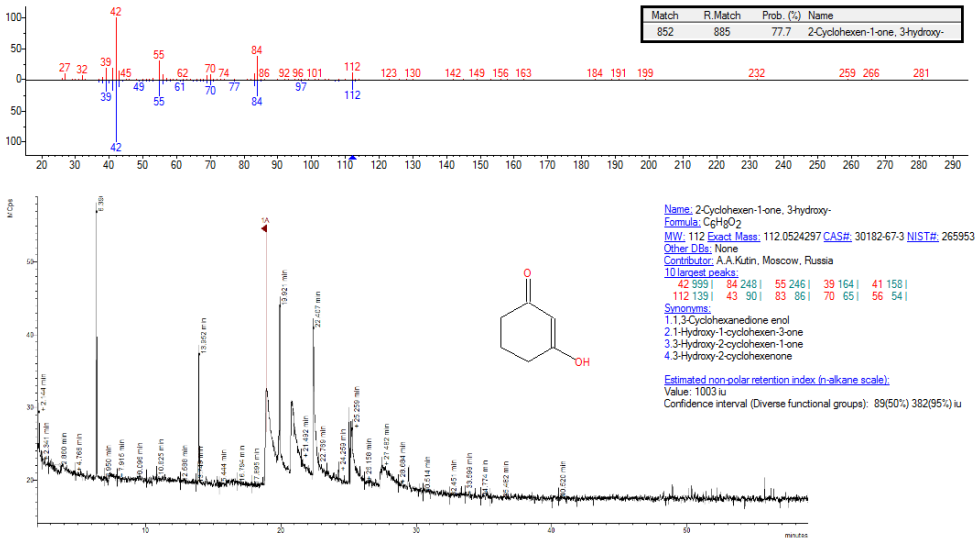

Fig. S4. Gas chromatography-mass spectrometry of hydroxyl-cyclohexene determined after prolonged reduction in a parallel-plate flow cell (–20 mA, –3.2 mA cm^{-2} for 100 h).

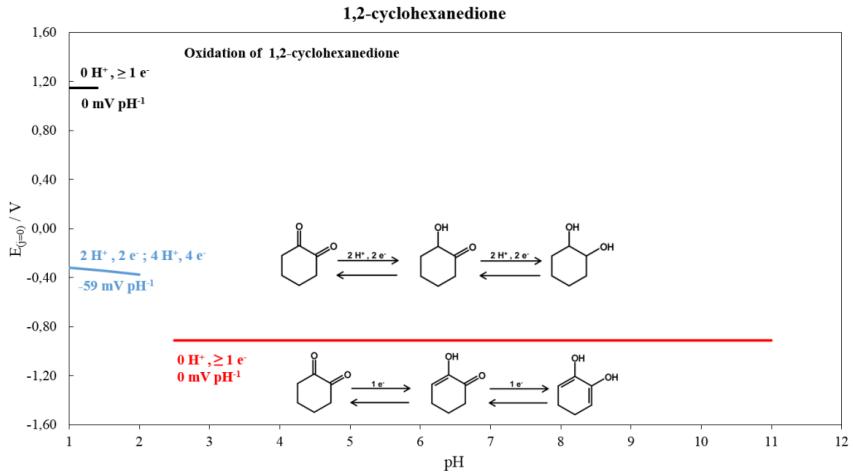

Figure S5 (a)

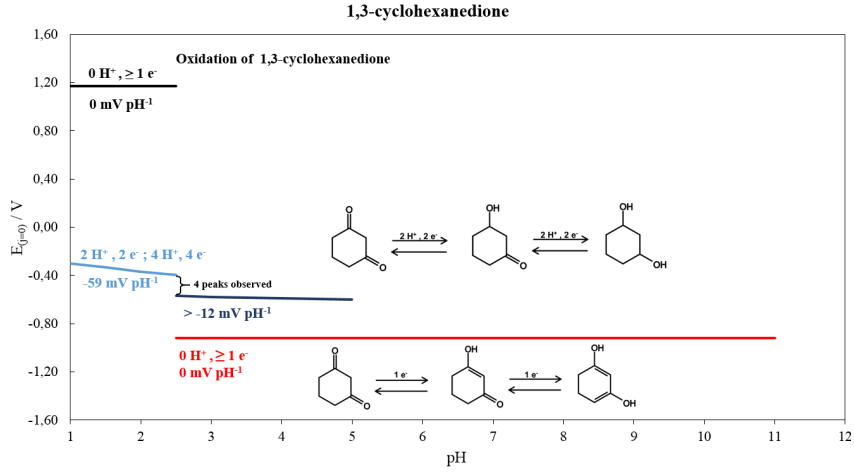

Figure S5 (b)

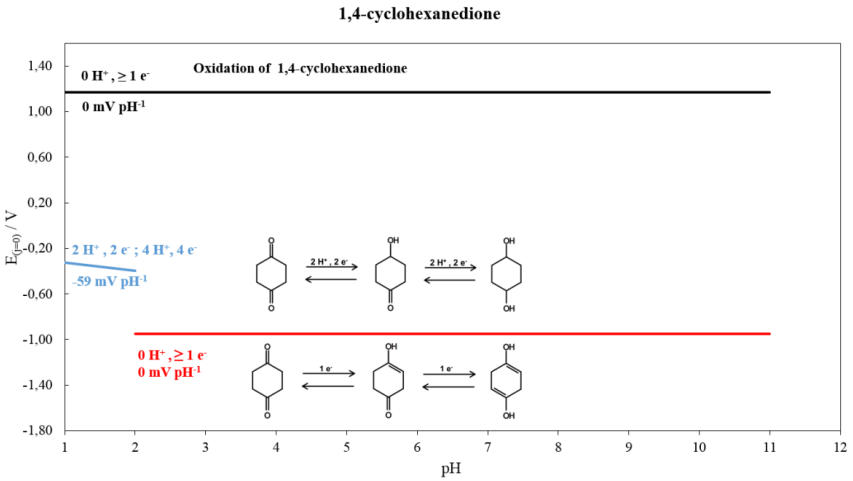

Figure S5 (c)

Fig. S5. *E_O vs*. pH plots of (a) 1,2-, (b) 1,3-, (c) 1, 4-cyclohexanedione molecules, extracted from the voltammetric data shown in Figure 5.

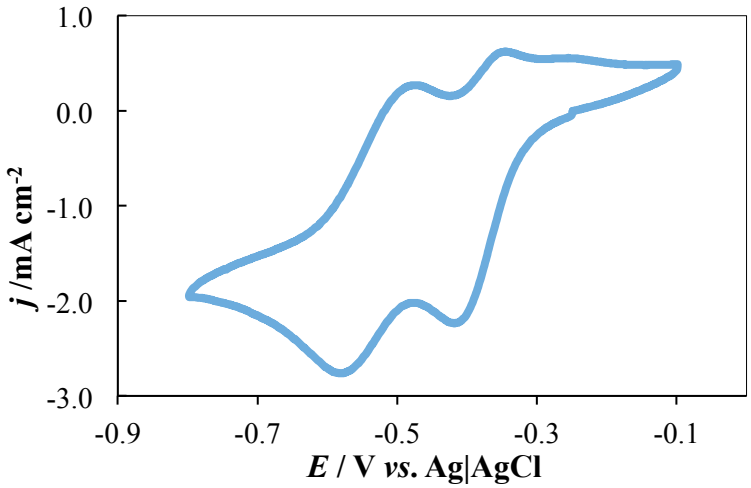

607

Fig. S6. Multi-electron transfers (n ≥ 2) observed in the cyclic voltammogram of 10 mmol dm^{-3} 1,3-cyclohexanedione and 0.2 mol dm^{-3} sodium chloride at pH 2.5 (Temperature = 25 °C, potential sweep rate: 100 mV s^{-1}).

608

609

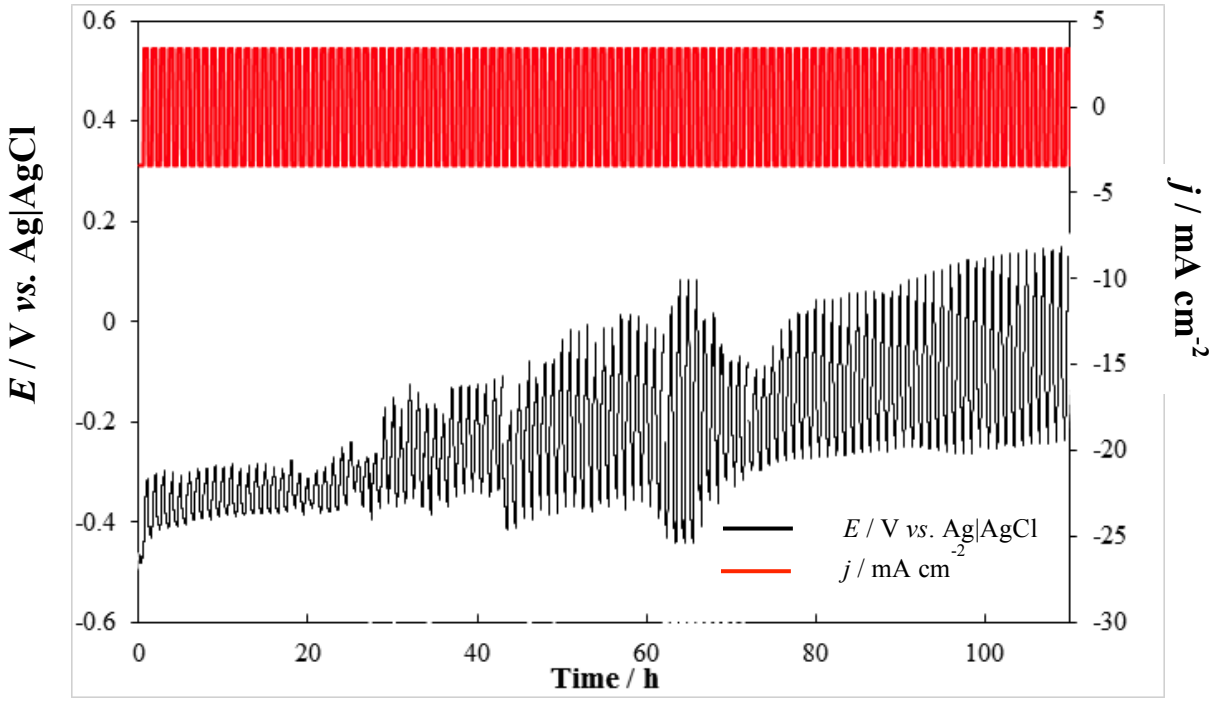

610

Fig. S7. The electrode potential *vs.* time response of the 1,3-cyclohexanedione half-cell reaction during an experiment using a 30 min charge – 30 min discharge regime at 20 mA (3.2 mA cm^{-2}) for 100 cycles.

611

612

613 **References**

[1]	M. R. Montoya, M.A. Zon, J.M.R. Mellado, Investigation of the reduction of 1, 2-cyclohexanedione and methylglyoxal on mercury electrodes under pure kinetic conditions by linear-sweep voltammetry, ***J. Electroanal. Chem.***, 1993, 353, 217 – 224.
[2]	M.A. Zon, J.M.R. Mellado, Study of the electrochemical reduction of unhydrated 1,2-cyclohexanedione on mercury electrodes, ***J. Electroanal. Chem***., 1992, 338, 229 – 238.
[3]	B. Yang, L. Hoober-Burkhardt, F. Wang, G.K. Surya Prakash, S.R. Narayanan, An Inexpensive Aqueous Flow Battery for Large-Scale Electrical Energy Storage Based on Water-Soluble Organic Redox Couples, ***J. Electrochem. Soc.***, 2014, 161, A1371– A1380.
[4]	T. Janoschka, N. Martin, U. Martin, C. Friebe, S. Morgenstern, H. Hiller, M.D. Hager, U.S. Schubert, An aqueous, polymer-based redox-flow battery using non-corrosive, safe, and low-cost materials, ***Nature***, 2015, 527, 78 – 81.
[5]	J.D. Milshtein, L. Su, C. Liou, A.F. Badel, F.R. Brushett, Voltammetry study of quinoxaline in aqueous electrolyte, ***Electrochim. Acta***, 2015, 180, 695 – 704.
[6]	K.X. Lin, Q. Chen, M.R. Gerhardt, L.C. Tong, S.B. Kim, L. Eisenach, A.W. Valle, D. Hardee, R.G. Gordon, M.J. Aziz, M.P. Marshak, Alkaline quinone flow battery, ***Science***, 2015, 349, 1529 – 1532.
[7]	K.X. Lin, R. Gomez-Bombarelli, E.S. Beh, L.C. Tong, Q. Chen, A. Valle, A. Aspuru-Guzik, M.J. Aziz, R.G. Gordon, A redox-flow battery with an alloxazine-based organic electrolyte, Nature Energy, 2016, 1, 16102

614

615

616